

Collision system size dependence of dihadron azimuthal correlations in ultra-relativistic heavy ion collisions

S. Zhang,¹ Y. H. Zhu,^{1,2} G. L. Ma,¹ Y. G. Ma*,¹ X. Z. Cai,¹ J. H. Chen,¹ and C. Zhong¹

¹*Shanghai Institute of Applied Physics, Chinese Academy of Sciences, Shanghai 201800, China*

²*Graduate School of the Chinese Academy of Sciences, Beijing 100080, China*

(Dated: October 24, 2018)

The system size dependence of dihadron azimuthal correlations in ultra-relativistic heavy ion collision is simulated by a multi-phase transport model. The structure of correlation functions and yields of associated particles show clear participant path-length dependences in collision systems with a partonic phase. The splitting parameter (D) and Root Mean Square Width ($\Delta\phi_{rms}$) of away side correlation functions increase with collision system size from $^{14}\text{N}+^{14}\text{N}$ to $^{197}\text{Au}+^{197}\text{Au}$ collisions. The double-peak structure of away side correlation functions can only be formed in sufficient “large” collision systems. These properties provide some hints to study onset of deconfinement, which is related to the QCD phase boundary and QCD critical point, by an energy-size scan.

PACS numbers: 25.75.Gz, 12.38.Mh, 24.85.+p

I. INTRODUCTION

Quantum Chromodynamics (QCD) calculation predicted an exotic quark-gluon matter in QCD phase diagram [1] may be created in the early stage of heavy ion collisions at ultra-relativistic energy [2]. For mapping the QCD phase diagram and locating QCD phase boundary and critical point [3], one needs to find a way to vary temperature, T , and chemical potential, μ_B . The NA61 collaboration and NA49-future collaboration [4] suggested that it can be achieved via a systematic energy (E) and system size (A) ($E-A$) scan. The present work focuses on the latter in different collision systems with partonic phase or hadron gas at $\sqrt{s_{NN}} = 200$ GeV.

Jet quenching phenomenon has been theoretically predicted [5] and experimentally observed [6]. So far, dihadron azimuthal correlation has been demonstrated as a good method to reconstruct particle and energy distribution induced by the quenched jet. In experiment, a double-peak structure was found on the away side of dihadron azimuthal correlation functions [9–11] and the indication of conical emission of charged hadrons was reported by the STAR collaboration [12]. A significant centrality dependence of double-peak structure of away-side correlation functions was observed by the PHENIX collaboration [11] and theoretically simulated in Ref. [13]. The centrality dependence results indicate that the structure of away-side correlation function is sensitive to system size of the reaction zone.

These interesting phenomena provoke some theorists into explaining the physical mechanisms for origins of the double-peak structure, such as Cherenkov-like gluon radiation model [14], medium-induced gluon bremsstrahlung radiation [15, 16], shock wave model in hydrodynamic equations [17], waking the colored plasma and sonic Mach

cones [18], sonic booms and diffusion wakes in thermal gauge-string duality [19], jet deflection [20] and strong parton cascade mechanism [13, 21–24].

All of the experimental and theoretical works suggest that the double-peak phenomenon is a good probe to study the hot and dense medium created in ultra-relativistic heavy ion collisions [7, 8]. In this paper we investigate the double-peak structure in different collision systems, namely $^{14}\text{N} + ^{14}\text{N}$, $^{16}\text{O} + ^{16}\text{O}$, $^{23}\text{Na} + ^{23}\text{Na}$, $^{27}\text{Al} + ^{27}\text{Al}$, $^{40}\text{Ca} + ^{40}\text{Ca}$, $^{64}\text{Cu} + ^{64}\text{Cu}$ and $^{197}\text{Au} + ^{197}\text{Au}$ at $\sqrt{s_{NN}} = 200$ GeV. The collision system size dependence of the double-peak structure of away-side correlation function is focused. We present participant path-length $\nu = 2N_{bin}/N_{part}$ [25] (N_{bin} and N_{part} are the number of binary collision and participants, respectively) dependence of the double-peak structure of away-side correlation function in the most central collisions (0-10%). In addition, the behavior of the away-side correlation function is also discussed at given various participant path-length $\nu \approx 1.90$ and 2.28. From these results, one can see that the structure of away-side correlation function changes near $^{40}\text{Ca} + ^{40}\text{Ca}$ collisions at $\sqrt{s_{NN}} = 200$ GeV in central collisions (0-10%), but there is no significant system dependence of the correlation at given participant path-length ν . These results show significant degree of freedom dependence in the system with a partonic phase or with a pure hadron gas [26], which provides potential information about the onset of deconfinement. This method supports the $E-A$ scan in experiment to investigate the QCD phase transition boundary and QCD critical point.

The paper is organized as follows. The following section introduces the model as well as the analysis method for dihadron azimuthal correlations. Section III describes the detailed results and discussions, which includes the structure of dihadron azimuthal correlation functions, yields and mean transverse momentum of associated particles, the splitting parameter (D) and $\Delta\phi_{rms}$ dispersion of away-side correlation functions and the corresponding results at given participant path-lengths. The nuclear

*Corresponding author: ygma@sinap.ac.cn

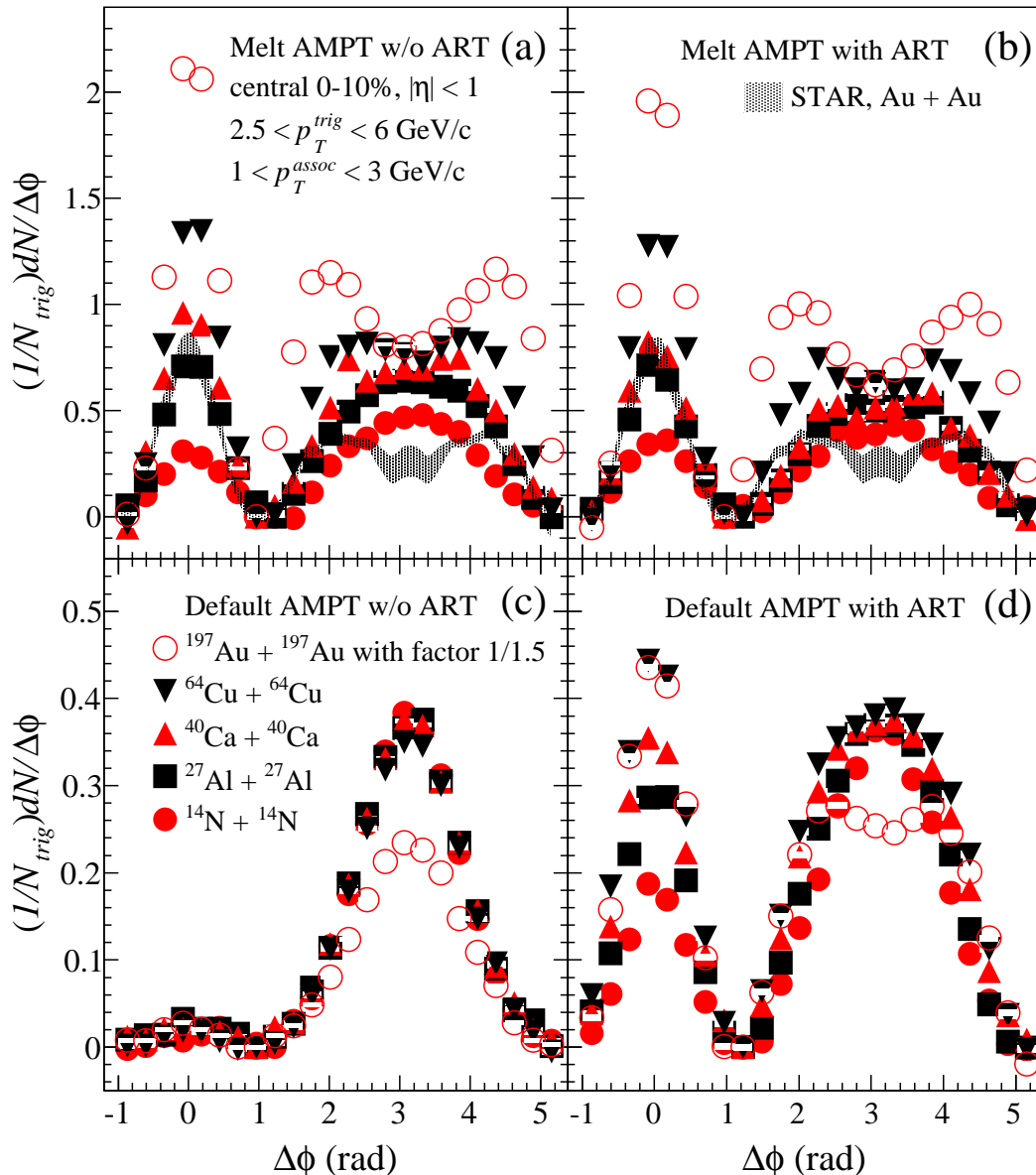


FIG. 1: (Color online) Dihadron azimuthal correlation functions for different collision systems in centrality 0-10% at $\sqrt{s_{NN}} = 200$ GeV; the shadowing area from the STAR data [9].

modification factor, R_{CP} , are also presented in Section III. Section IV gives a summary.

II. MODEL AND ANALYSIS METHOD

In this paper, a multi-phase transport model (AMPT) [27], which is a hybrid model, is employed to study dihadron azimuthal correlations. It includes four main components to describe the physics in relativistic heavy ion collisions: 1) the initial conditions from HIJING model [28], 2) partonic interactions modeled by

a Parton Cascade model (ZPC) [29], 3) hadronization (discussed later), 4) hadronic rescattering simulated by A Relativistic Transport (ART) model [30]. Excited strings from HIJING are melted into partons in the AMPT version with string melting mechanism [31] (abbr. ‘*the Melt AMPT version*’) and a simple quark coalescence model is used to combine the partons into hadrons. In the default version of AMPT model [32] (abbr. ‘*the Default AMPT version*’), minijet partons are recombined with their parent strings when they stop interactions and the resulting strings are converted to hadrons via the Lund string fragmentation model [33]. The Melt AMPT ver-

sion undergoes a partonic phase, while a pure hadron gas is in the Default AMPT version. Details of the AMPT model can be found in a review paper [27] and previous works [27, 31, 34].

The analysis method for dihadron azimuthal correlations is similar to that used in previous experiments [8, 10], which describes the azimuthal correlation between a high p_T particle (trigger particle) and low p_T particles (associated particles). The raw signal can be obtained by accumulating pairs of trigger and associated particles into $\Delta\phi = \phi_{assoc} - \phi_{trig}$ distributions in the same event. The background which is expected mainly from elliptic flow is simulated by mixing event method [8, 10]. By selecting the associated particles in different events whose centralities are every close to that of the same event (raw signals), the $\Delta\phi$ distribution can be obtained as the corresponding background. The background is subtracted from raw signal by using A Zero Yield At Minimum (ZYAM) assumption as that used in experimental analysis [10] (See our detailed analysis in Ref. [13]).

III. RESULTS AND DISCUSSIONS

A. Structure of dihadron correlation function

The participant path-length, defined as $\nu = 2N_{bin}/N_{part}$ [25], can describe degree of multiple collisions between participants in the early stage of heavy ion collisions and characterize the size of the reaction zone. The n_{col}^{parton} represents average collision number of partons in the Melt AMPT version. The values of ν and n_{col}^{parton} significantly increase with varying collision system ($CSYS$) from “small” size to “large” size at $\sqrt{s_{NN}} = 200$ GeV in the most central collisions (0-10%) as shown in Table I. From this table, we can see the multiple collisions are more enhanced in “large” size collision system than in “small” size one. The values of N_{part} , N_{bin} and ν are comparable to those from the Glauber Model [35] for both $^{64}\text{Cu} + ^{64}\text{Cu}$ and $^{197}\text{Au} + ^{197}\text{Au}$ collisions.

Figure 1 shows dihadron azimuthal correlation functions of different collision systems in the most central (0-10%) collisions at $\sqrt{s_{NN}} = 200$ GeV. The correlation functions are calculated in the kinetic windows, $1 < p_T^{assoc} < 3$ GeV/ c as well as $2.5 < p_T^{trig} < 6$ GeV/ c and $|\eta| < 1$. It shows that the structure of away-side correlation function changes from the Gaussian-like distribution to double-peak structure, obviously emerging in $^{40}\text{Ca} + ^{40}\text{Ca}$ collisions, with varying collision system from $^{14}\text{N} + ^{14}\text{N}$ to $^{197}\text{Au} + ^{197}\text{Au}$ collisions in the Melt AMPT version. In this figure, the amplitude of the correlation function becomes higher with the increasing of collision system size. The associated particles in the Melt AMPT version are more abundant than those in the Default AMPT version.

The yields of associated particles on near-side correlation functions from the Default AMPT version without hadronic rescattering is very small. The jet pair from HI-

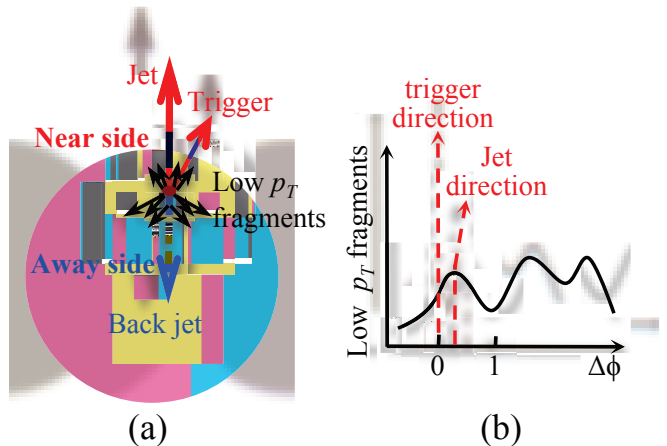


FIG. 2: (Color online) Schematic illustrations, (a) fragments from jet in relativistic heavy ion collisions, (b) azimuthal correlations between trigger particle and low p_T fragments.

JING [28] keeps momentum conservation law and number of particles from jet fragmentation dose not balance on the near side and away side, which was investigated in p + p collisions [36]. In the Default AMPT version without hadronic rescattering, the Gaussian-shaped fragments around the jet direction are emitted from the jet, while the trigger particle in the fragments are not always along the direction of the jet, a schematic illustration shown in panel (a) of Fig 2. The azimuthal correlations between trigger particle and low p_T fragments can be obtained in panel (b) in Fig 2. The near-side peak are around direction of near-side jet and shifts from direction of trigger particle in some cases. As an integral result, the amplitude of near side will be very small in the Default AMPT version without hadronic rescattering.

It is obvious that hadronic rescattering enhances the correlation on the near side and broadens the structure on the away side in the Default AMPT version. As we have already demonstrated, the structure of dihadron correlation functions is more reasonable in the Melt AMPT version than in the Default AMPT version [13]. However the Default AMPT version is used to compare the properties of the double-peak structure in partonic phase and in hadron gas, especially for “small” size collision system. For investigating the properties of collision system size dependences of away-side dihadron azimuthal correlations, we extract the associated particle yield N_{away}^{assoc} , splitting parameter (D) (half distance between double peaks on the away side), Root Mean Square Width ($\Delta\phi_{rms}$) and mean transverse momentum $\langle p_T \rangle_{away}^{assoc}$ of away-side associated particles, which will be discussed later, respectively.

TABLE I: $N_{part}(CSYS)$, $N_{bin}(CSYS)$, $\nu(CSYS) = \frac{2N_{bin}(CSYS)}{N_{part}(CSYS)}$, n_{col}^{parton} in different collision system at $\sqrt{s_{NN}} = 200$ GeV for centrality 0-10 %, the value in blanket is taken from Glauber Model [35].

$CSYS$	$^{14}\text{N} + ^{14}\text{N}$	$^{16}\text{O} + ^{16}\text{O}$	$^{23}\text{Na} + ^{23}\text{Na}$	$^{27}\text{Al} + ^{27}\text{Al}$	$^{40}\text{Ca} + ^{40}\text{Ca}$	$^{64}\text{Cu} + ^{64}\text{Cu}$	$^{197}\text{Au} + ^{197}\text{Au}$
$N_{part}(CSYS)$	20.78	24.25	35.92	43.61	65.97	107.04 (99.0)	343.32 (325.9)
$N_{bin}(CSYS)$	19.63	23.69	41.01	54.34	91.15	179.98 (188.8)	914.71 (939.4)
$\nu(CSYS) = \frac{2N_{bin}(CSYS)}{N_{part}(CSYS)}$	1.89	1.95	2.28	2.49	2.76	3.36 (3.8)	5.33 (5.7)
n_{col}^{parton}	1.31	1.44	1.93	2.23	2.79	3.80	7.24

B. Yield of associated particles

The $\nu(CSYS)$ dependence of N_{away}^{assoc} is shown in Fig. 3 from the Melt/Default AMPT version, respectively. It presents a significant increasing trend of N_{away}^{assoc} with varying the collision system from $^{14}\text{N} + ^{14}\text{N}$ to $^{197}\text{Au} + ^{197}\text{Au}$ collisions in the most central collisions (0-10%) at $\sqrt{s_{NN}} = 200$ GeV in the Melt AMPT version. The Default AMPT version, with a hadronic gas, does not result in a rapidly increasing dependence trend. In the Melt AMPT version, the dependence trend indicates the jet correlation information can be inherited by more particles in a partonic phase than in a hadronic gas, especially in “large” size collision system. Furthermore it implies that the interaction strength in “large” size collision system is more significant than that in “small” size collision system, and while strong parton cascade plays a dominant role in dihadron azimuthal correlations in the Melt AMPT version. It is interesting that the increasing slope of N_{away}^{assoc} vs $\nu(CSYS)$ from the linear fitting in the Melt AMPT version is quicker after $^{40}\text{Ca} + ^{40}\text{Ca}$ collision system, where clear double-peak structure emerges, than that in small systems. This property indicates the double-peak (Mach-like) structure can enhance associated particles yields of jet correlations partially.

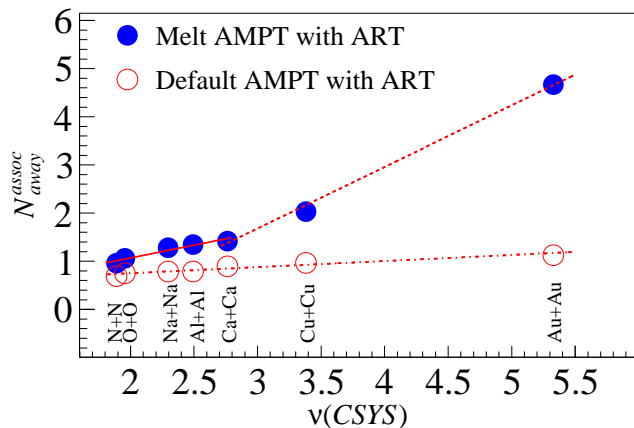


FIG. 3: (Color online) Yield of associated particles on away-side correlation functions, N_{away}^{assoc} , as a function of $\nu(CSYS)$ by the Melt/Default AMPT version in centrality 0-10% at $\sqrt{s_{NN}} = 200$ GeV.

C. $\Delta\phi_{rms}$ and splitting parameter on the away side

Root Mean Square Width ($\Delta\phi_{rms}$) of away-side correlation function is defined as

$$\Delta\phi_{rms} = \sqrt{\frac{\sum_{away} (\Delta\phi - \Delta\phi_m)^2 (1/N_{trig})(dN/d\Delta\phi)}{\sum_{away} (1/N_{trig})(dN/d\Delta\phi)}},$$

where $\Delta\phi_m$ is the mean $\Delta\phi$ of away-side correlation function and it approximates to π . $\Delta\phi_{rms}$ can describe broadening of away-side correlation function relative to π which is direction of back jet. By $\Delta\phi_{rms}$, one can investigate diffusion degree of the associated particles relative to back jet. The $\nu(CSYS)$ dependences of $\Delta\phi_{rms}$ in the Melt/Default AMPT version are shown in Fig. 4, respectively. $\Delta\phi_{rms}$ from the Melt AMPT version are consistent with PHENIX data [10, 37] in Cu + Cu and Au + Au collisions. $\Delta\phi_{rms}$ increases from $^{14}\text{N} + ^{14}\text{N}$ collisions to $^{197}\text{Au} + ^{197}\text{Au}$ collisions in the Melt AMPT version and the increasing trend is not so quick in the Default AMPT version. The increasing trend of $\Delta\phi_{rms}$ shows broadening of away-side correlation functions with increasing size of collision system. It indicates that the jet correlation information can reach faraway relative to direction of jet with changing the collision system from “small” size one to “large” size in a partonic phase. It is remarkable that the increasing trend of $\Delta\phi_{rms}$ from the linear fitting in the Melt AMPT version shows two different slope after and before $^{40}\text{Ca} + ^{40}\text{Ca}$ collision system, where clear double-peak structure emerges. This interesting result indicates that the double-peak (Mach-like) phenomenon from quenched-jet pushes evolution of jet correlations. At given $\nu(CSYS)$ case, we investigate system dependence of the double-peak structure in the Melt AMPT version. The $\Delta\phi_{rms}$ keeps a flat pattern with varying collision system in Fig. 6 at given $\nu(CSYS) \approx 1.9$ and 2.28. The $\Delta\phi_{rms}$ independence of collision system at given $\nu(CSYS)$ implies that the broadening of the away-side correlation function is only sensitive to how violent interactions in collision system, which determines how far the jet correlation information spreads. These results suggest that the back jet modification in the medium created in heavy ion collisions with a partonic phase is more obvious in the “large” size collision system than in “small” size one.

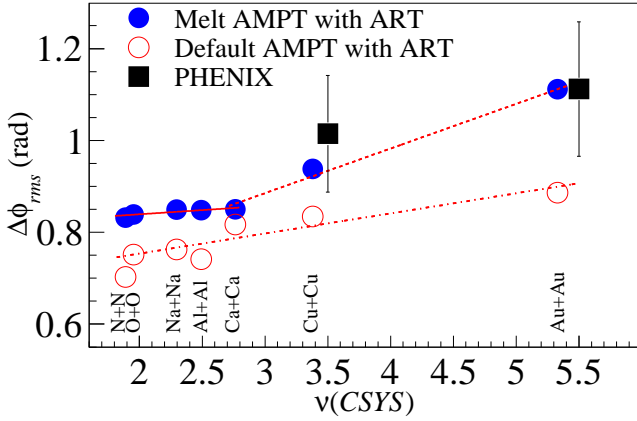


FIG. 4: (Color online) $\Delta\phi_{rms}$ of the away-side correlation functions as a function of $\nu(CSYS)$ in the Melt/Default AMPT version for the centrality 0-10% at $\sqrt{s_{NN}} = 200$ GeV; Square from PHENIX data [10, 37].

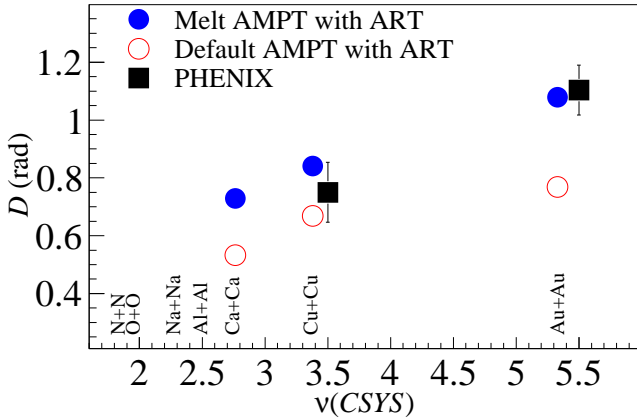


FIG. 5: (Color online) Splitting parameter (D) of the away-side correlation functions as a function of $\nu(CSYS)$ in the Melt/Default AMPT version for the centrality 0-10% at $\sqrt{s_{NN}} = 200$ GeV; Square from PHENIX data [11].

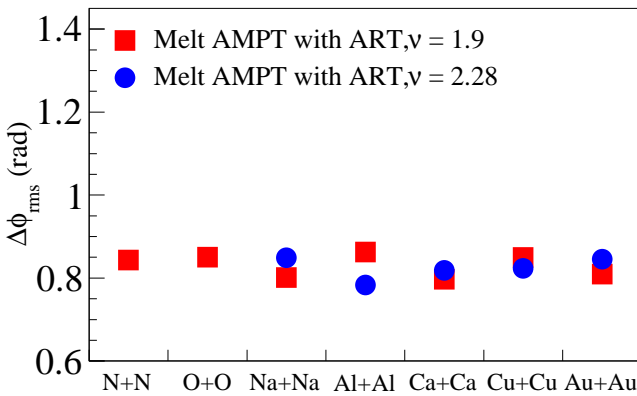


FIG. 6: (Color online) $\Delta\phi_{rms}$ on away-side of the correlation functions at given $\nu(CSYS) \approx 1.90, 2.28$ at $\sqrt{s_{NN}} = 200$ GeV.

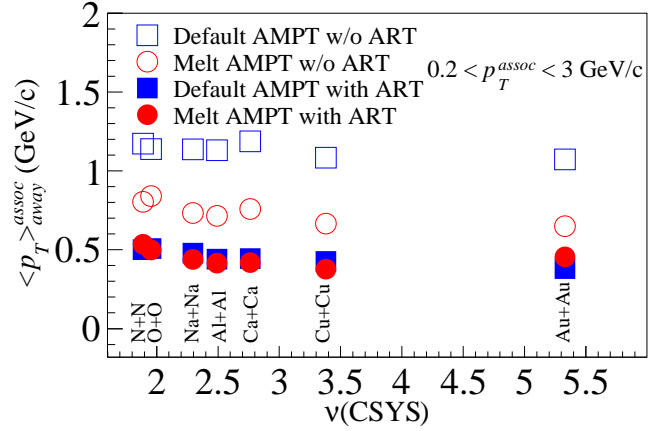


FIG. 7: (Color online) Mean transverse momentum ($\langle p_T \rangle_{away}^{assoc}$) of the away-side correlation functions as a function of $\nu(CSYS)$ in the Melt/Default AMPT version in centrality 0-10% at $\sqrt{s_{NN}} = 200$ GeV.

The splitting parameter (D) is another useful observable to characterize the structure of the double-peak of away-side correlation function, and further discloses essential of jet modification. The $\nu(CSYS)$ dependence of splitting parameter (D) in the Melt/Default AMPT version are shown in Fig. 5, respectively, in the most central collisions at $\sqrt{s_{NN}} = 200$ GeV. Double Gaussian function is not used to fit away-side correlation functions since there is no obvious double-peak structure from in $^{14}\text{N} + ^{14}\text{N}$ to in $^{27}\text{Al} + ^{27}\text{Al}$ collisions. The splitting parameter (D) increases from “small” size collision system to “large” size one in the Melt AMPT version. It is obvious that the splitting parameter (D) is smaller in the Default AMPT version than in the Melt AMPT version. The results in the Melt AMPT version are comparable to PHENIX data [11] in Cu + Cu and Au + Au collisions due to effect of parton cascade in the Melt AMPT version [13]. The parton interaction cross section is taken to be 10 mb, which is reasonable for reproducing elliptic flow and dihadron azimuthal correlations in the Melt AMPT version [13, 27, 31, 34]. In addition, Reference [6] demonstrated that there is a strong suppression of inclusive yield and back-to-back correlations at high p_T in $^{197}\text{Au} + ^{197}\text{Au}$ collisions relative to that in $\text{d} + ^{197}\text{Au}$ collisions at $\sqrt{s_{NN}} = 200$ GeV. Theoretical studies suggest that the emission angle relative to jet should be about 1.23 rad for QGP, 1.11 rad for hadronic gas and zero for mixed phase [17]. The radiation mechanism for the double-peak structure [14] suggests the more energetic jet, the smaller the emission angle. And in this calculation it indicates the double-peak structure is more obvious in a partonic phase than in a hadron gas. A quick change of the double-peak structure is expected while one experimentally scan the system size or beam energy near the QCD critical point or phase transition boundary. It implies that the double-peak structure and jet modification is sensitive to the effective degree of free-

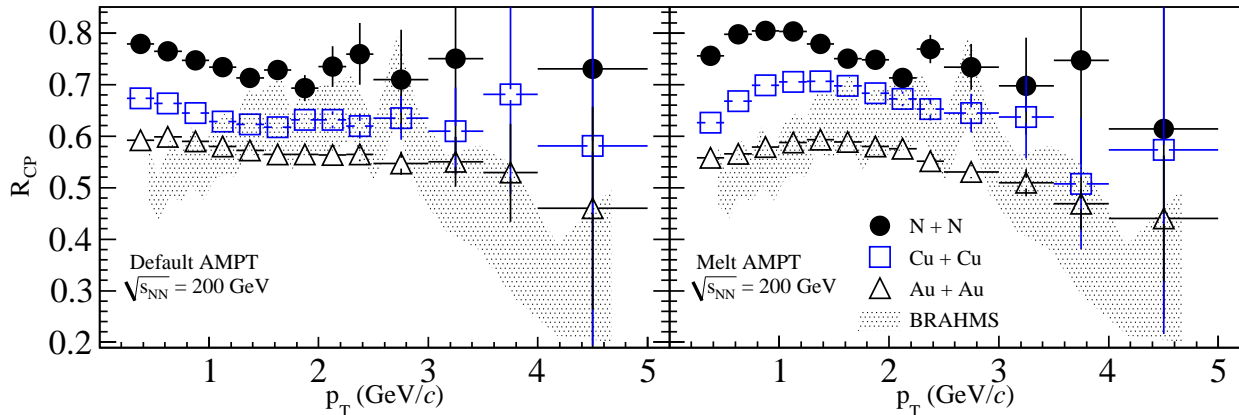


FIG. 8: (Color online) R_{CP} in the Default AMPT Version at $\sqrt{s_{NN}} = 200$ GeV, the shadowing from BRAHMS data [38] in Au + Au collisions.

dom of the dense medium created in heavy ion collisions, which is related to onset of deconfinement.

From these results, it can be concluded that a considerable “large” collision system is necessary and the strong parton cascade is important for forming the double-peak structure of away-side correlation function. An onset of the obvious double-peak structure takes place around the collision mass range near $^{40}\text{Ca} + ^{40}\text{Ca}$ collisions. This phenomenon indicates that the correlation is sensitive to $\nu(CSYS)$ and n_{col}^{parton} , i.e. the correlation depends on the collision system size and the violent degree of the partonic interaction in a partonic phase. The results in different group in a parton phase and a pure hadron gas imply the correlations are sensitive to the effective degree of freedom of the dense medium created in relativistic heavy ion collisions, which can give us some hints of the onset of deconfinement in the system-size viewpoint.

D. Mean transverse momentum of associated particles in central collisions

For further investigating the contribution of parton cascade and hadronic rescattering to jet modification, we calculate mean transverse momentum of away-side associated particles in central collisions at $\sqrt{s_{NN}} = 200$ GeV and $\langle p_T \rangle^{assoc}$ is fixed at (0.2, 3) GeV/c. $\langle p_T \rangle^{assoc}$ is presented as a function of $\nu(CSYS)$ in the Melt/Default AMPT version with/without hadronic rescattering in Fig. 7, respectively. $\langle p_T \rangle^{assoc}$ slightly decreases with varying collision system from “small” size to “large” size one. $\langle p_T \rangle^{assoc}$ for different systems are higher in the Default AMPT version without hadronic rescattering than in other case. And $\langle p_T \rangle^{assoc}$ are at the bottom and no difference in the Melt AMPT/Default AMPT version with hadronic rescattering. The results in the Melt AMPT version without hadronic rescattering are between them. These results are consistent with what we discussed in the introduction to AMPT model. The initial condition for AMPT is from HIJING [28], corresponding to the

AMPT without parton cascade and hadronic rescattering, so we get the high $\langle p_T \rangle^{assoc}$ in this case. And the particles will be softened by parton cascade and hadronic rescattering. The condition for hadronic rescattering is sensitive to how close the distance between hadrons is in hadronic rescattering (ART) [30]. In the Melt AMPT version, the system undergoes parton cascade with expansion of the system and then partons are combined into hadrons. However in the Default AMPT version, the system skips the parton cascade stage and most of hadrons can participate in hadronic rescattering. Therefore hadronic rescattering contribution is more significant in the Default AMPT version than in the Melt AMPT version.

E. Suppression of high- p_T hadrons

Jet-quenching can be investigated by dihadron azimuthal correlations as discussed above. Another important phenomenon about jet-quenching is suppression of high- p_T hadrons in relativistic heavy ion collisions. The nuclear modification factor, R_{cp} , describes this phenomenon, defined as,

$$R_{CP} = \frac{\frac{d^2N}{p_T dp_T d\eta}(Central)/N_{bin}(Central)}{\frac{d^2N}{p_T dp_T d\eta}(Peripheral)/N_{bin}(Peripheral)},$$

where the central and peripheral collision centralities are, respectively, 0-10% and 40-60%. Figure 8 shows the R_{CP} calculated in the Melt AMPT version (right panel) and in the Default AMPT version (left panel) in relativistic heavy ion collisions at $\sqrt{s_{NN}} = 200$ GeV. To clearly see the system size dependence, we present R_{CP} in $^{14}\text{N} + ^{14}\text{N}$, $^{64}\text{Cu} + ^{64}\text{Cu}$ and $^{197}\text{Au} + ^{197}\text{Au}$ collisions and those in other collision systems keep the similar dependent trend. The shadowing area in this figure is from BRAHMS data [38]. The hadrons in the Melt AMPT version, which undergo a partonic phase, are suppressed at high p_T and those from the Default AMPT version, in

a hadron gas, are not suppressed obviously. The R_{CP} in $^{197}\text{Au} + ^{197}\text{Au}$ collisions from the Melt AMPT version is consistent with the experimental data [38]. We can conclude that there is jet-quenching-like mechanism in the system with partonic phase and jet-quenching phenomenon is more obvious in the “large” size collision system than in “small” size one.

IV. SUMMARY

In summary, the present paper discusses the collision system size dependences of dihadron azimuthal correlations at $\sqrt{s_{NN}} = 200$ GeV by a multi-phase transport model. It presents the properties of away-side correlation functions, such as N_{assoc}^{away} , $\Delta\phi_{rms}$, D and $\langle p_T^{away} \rangle$. The onset of obvious double-peak structure occurs near $^{40}\text{Ca} + ^{40}\text{Ca}$ collisions and away-side correlation function becomes more and more broadening with the increasing of collision system size. The yields of associated parti-

cles (N_{assoc}^{away}), $\Delta\phi_{rms}$ of away-side correlation functions and splitting parameter (D) show significant system size dependences. These results also present the degree of freedom dependence, which is related to onset of deconfinement. The present analysis may shed light on the QCD phase boundary and critical point in experiment by the energy-size scan.

Acknowledgements

This work was supported in part by the National Natural Science Foundation of China under Grant No. 10979074, 10705043, 10705044, 10775167 and 10875159, and the Shanghai Development Foundation for Science and Technology under contract No. 09JC1416800, and the Knowledge Innovation Project of the Chinese Academy of Sciences under Grant No. KJCX2-YW-A14 and O95501P011 and the Project-sponsored by SRF for ROCS, SEM. O819011012.

-
- [1] Frank R. Brown et al., Phys. Rev. Lett. **65**, 2491 (1990).
 [2] I. Arsene et al., Nucl. Phys. **A757**, 1 (2005); B. B. Back et al. (PHOBOS Collaboration), *ibid.* **A757**, 28 (2005); J. Adams et al. (STAR Collaboration), *ibid.* **A757**, 102 (2005); S. S. Adcox et al. (PHENIX Collaboration), *ibid.* **A757**, 184 (2005).
 [3] Mark G. Alford et al., hep-ph/07094635; Frithjof Karsch, Nucl. Phys. A **698**, 199c (2002).
 [4] A. Laszlo et al. (NA61 Collaboration), PoS CPOD07:054, 2007; M. Gazdzicki et al. (The NA49-future Collaboration), arXiv:nucl-ex/0612007.
 [5] M. Gyulassy and M. Plümer, Phys. Lett. B **243**, 432 (1990); X. N. Wang and M. Gyulassy, Phys. Rev. Lett. **68**, 1480 (1992); R. Baier, D. Schiff, and B.G. Zakharov, Ann. Rev. Nucl. Part. Sci. **50**, 37 (2000).
 [6] C. Adler et al. (STAR Collaboration), Phys. Rev. Lett. **91**, 072304 (2003); J. Adams et al. (STAR Collaboration), Phys. Rev. C **73**, 064907 (2006); J. Adams et al. (STAR Collaboration), J. Phys. G **34**, 799 (2007); S. S. Adler et al. (PHENIX Collaboration), Phys. Rev. Lett. **91**, 072301 (2003); S. S. Adler et al. (PHENIX Collaboration), Phys. Rev. C **73**, 054903 (2006); S. S. Adler et al. (PHENIX Collaboration), Phys. Rev. C **71**, 051902 (2005).
 [7] C. Adler et al. (STAR Collaboration), Phys. Rev. Lett. **90**, 082302 (2003).
 [8] J. Adams et al. (STAR Collaboration), Phys. Rev. Lett. **95**, 152301 (2005).
 [9] J. G. Ulery (STAR Collaboration), Nucl. Phys. A **774**, 581 (2006).
 [10] S.S. Adler et al. (PHENIX Collaboration), Phys. Rev. Lett. **97**, 052301 (2006).
 [11] Jiangyong Jia (PHENIX Collaboration), arXiv:nucl-ex/0510019.
 [12] B.I. Abelev et al. (STAR Collaboration), Phys. Rev. Lett. **102**, 052302 (2009); Claude A. Pruneau et al., J. Phys. G: Nucl. Part. Phys. **34**, S667 (2007).
 [13] G. L. Ma, S. Zhang, Y. G. Ma et al., Phys. Lett. B **641**, 362 (2006).
 [14] V. Koch, A. Majumder, Xin-Nian Wang, Phys. Rev. Lett. **96**, 172302 (2006).
 [15] I. Vitev, Phys. Lett. B **630**, 78 (2005).
 [16] A. D. Polosa and C. A. Salgado, Phys. Rev. C **75**, 041901 (R) (2007).
 [17] J. Casalderrey-Solana et al., J. Phys. Conf. Ser. **27**, 22 (2005); Nucl. Phys. A **774**, 577 (2006).
 [18] J. Ruppert, B. Müller, Phys. Lett. B **618**, 123 (2005); R. B. Neufeld, B. Muller and J. Ruppert, Phys. Rev. C **78**, 041901 (2008).
 [19] Steven S. Gubser, Silviu S. Pufu, Phys. Rev. Lett. **100**, 012301 (2008).
 [20] Néstor Armesto, Carlos A. Salgado, and Urs Achim Wiedemann, Phys. Rev. C **72**, 064910 (2005).
 [21] G. L. Ma, Y. G. Ma, S. Zhang et al., Phys. Lett. B **647**, 122 (2007).
 [22] G. L. Ma, S. Zhang, Y. G. Ma et al., arXiv:nucl-th/0610088.
 [23] S. Zhang, G. L. Ma, Y. G. Ma et al., Phys. Rev. C **76**, 014904 (2007).
 [24] G. L. Ma, talk and proceeding for Strangeness in Quark Matter 2009.
 [25] W. Busza et al. Phys. Rev. Lett. **34**, 836 (1975); T. A. Trainor and Duncan J. Prindle, hep-ph/0411217; T. A. Trainor, arXiv:0710.4504.
 [26] S. Zhang, J. H. Chen, H. Crawford, D. Keane, Y. G. Ma, Z. B. Xu, Phys. Lett. B **684**, 224 (2010).
 [27] Z. W. Lin, C. M. Ko, B. A. Li, B. Zhang, S. Pal, Phys. Rev. C **72**, 064901 (2005).
 [28] X.-N. Wang and M. Gyulassy, Phys. Rev. D **44**, 3501 (1991); M. Gyulassy and X.-N. Wang, Comput. Phys. Commun. **83**, 307 (1994).
 [29] B. Zhang, Comput. Phys. Commun. **109**, 193 (1998).
 [30] B. A. Li and C. M. Ko, Phys. Rev. C **52**, 2037 (1995).
 [31] Z.W. Lin, C. M. Ko, Phys. Rev. C **65**, 034904 (2002); Z. W. Lin, C. M. Ko et al., Phys. Rev. Lett. **89**, 152301

- (2002).
- [32] B. Zhang, C. M. Ko et al., Phys. Rev. C **61**, 067901 (2000).
- [33] B. Andersson, G. Gustafson et al., Phys. Rep. **97**, 31 (1983).
- [34] J. H. Chen, Y. G. Ma, G. L. Ma et al., Phys. Rev. C **74**, 064902 (2006).
- [35] B. I. Abelev et al. (STAR Collaboration), Phys. Lett. B **673**, 183 (2009).
- [36] K. F. Xin, S. Zhang et al., Chin. Phys. Lett. **26**, 062503 (2009).
- [37] W. G. Holzmann (PHENIX Collaboration), nucl-ex/0608030.
- [38] I. Arsene et al. (BRAHMS Collaboration), Phys. Rev. Lett. **91**, 072305 (2003).